NUMERICAL SIMULATIONS OF PLANETESIMAL COLLISIONS: THE RELATIONSHIP BETWEEN IMPACT CONDITIONS AND RESULTANT SHAPES.
Keisuke Sugiura[1], Hiroshi Kobayashi[1], and Shu-ichiro Inutsuka[1]; [1]Graduate School of Science, Nagoya University, Aichi, Japan (sugiura.keisuke@a.mbox.nagoya-u.ac.jp).

Introduction: Planets are formed through collisional coalescence of planetesimals, which have the typical radius from km to 100 km. The early phase of collisional growth of planetesimals is supposed to be in “runaway” mode, that is, larger planetesimals grow more rapidly than smaller ones. Thus smaller planetesimals mainly remain as asteroids in the present solar system, and they are expected to record information of the past collisional history.

Shapes of asteroids are distinctly different from spheres, such as the sea-otter shape of asteroid Itokawa. Irregular shapes are probably formed through collisional destruction of planetesimals and subsequent gravitational reaccumulation. The relationship between shapes of collisional outcomes and impact conditions (e.g., impact angles and velocities) reveals impact conditions to form shapes of existing asteroids, and this may lead to collisional history in the solar system.

Method: To reproduce collisions between planetesimals, we conduct numerical simulations with Smoothed Particle Hydrodynamics (SPH) method for elastic dynamics [1]. We include the self-gravity, a model of fracture for brittle solid [2] and friction between completely damaged rock [3] to treat collisional destruction and shape formation through reaccumulation of fragments. For fast calculation of impact simulations, we parallelize our simulation code using Framework for Developing Particle Simulator (FDPS) [4,5].

Impact Conditions: We model colliding planetesimals as a sphere of basalt with the radius of 50 km and zero rotation. We use 50,000 SPH particles for a planetesimal. Here, we focus on collisions between two equal-mass planetesimals. We vary the impact velocity v_{imp} from 50 m/s to 400 m/s with the increment of 25 m/s, and the impact angle θ_{imp} from 5° to 45° with the increment of 5°. We conduct totally 135 impact simulations with each impact velocity and angle until about 1 day after the impact. The definitions of the impact velocity and angle are following those of [6].

Results: Figure 1 shows the snapshots of the SPH simulation with v_{imp} = 200 m/s and θ_{imp} = 15°. As a result of this impact, spherical planetesimals are completely deformed by the impact (Fig. 1 b, c) , and the elongated shape of the largest remnant is formed through gravitational reaccumulation of fragments (Fig. 1 d, e).

Depending on the impact velocity and angle, various shapes of the largest remnants are formed. Fig. 2 shows typical shapes observed in our simulations. Each typical shape is mainly formed through impacts with following impact velocities and angles: v_{imp} ~ 50 m/s (bilobed shapes), v_{imp} ~ 100 m/s and θ_{imp} < 20° (spherical shapes), v_{imp} > 100 m/s and θ_{imp} < 10° (flat shapes), v_{imp} > 100 m/s and 10° < θ_{imp} < 30° (elongated shapes), v_{imp} > 100 m/s and 30° < θ_{imp} (hemispherical shapes).

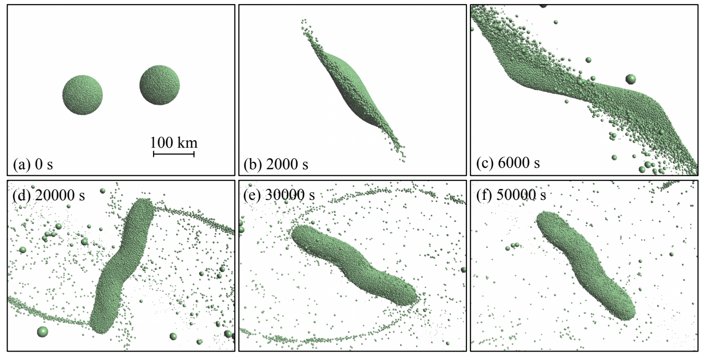

Figure 1: The snapshots of the impact simulation with v_{imp} = 200 m/s and θ_{imp} = 15° at 0 s(a), 2000 s(b), 6000 s(c), 20000 s(d), 30000 s(e), and 50000 s(f).

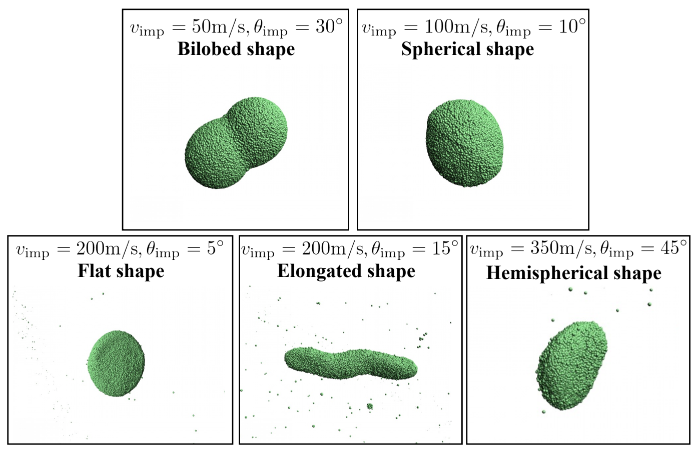

Figure 2: Typical shapes of the largest remnant formed in our simulations.

To evaluate shapes of the largest remnant quantitatively, we measure axis ratios of the largest remnants using inertia moment. Based on values of two axis ratios (ratio of intermediate/major axis length and minor/major axis length) and mass of the largest remnant M_{lr}, we classify shapes into five categories shown in Fig. 2. Note that if M_{lr} is smaller than 0.4 of mass of the initial planetesimal M_{target}, we do not classify shapes for such destructive impacts because the number of SPH particle to resolve the largest remnant is insufficient. Figure 3 shows the result of classification.

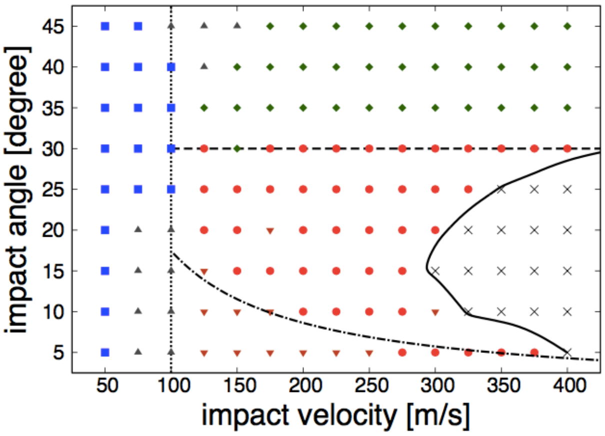

Figure 3: The result of classification of shapes of the largest remnants formed by each impact simulation. Blue squares show bilobed shapes, gray triangles show spherical shapes, brown inverted triangles show flat shapes, red circles show elongated shapes, green diamonds show hemispherical shapes, and black crosses show impacts with $M_{lr}/M_{target} < 0.4$. Dotted line shows v_{imp} = 100 m/s, dashed line shows θ_{imp} = 30°, chain curve shows $v_{imp}\sin\theta_{imp}$ = 30 m/s, and solid curve shows $M_{lr}/M_{target} = 0.4$.

Discussion: Based on the result of shape classification shown in Fig. 3, we find four conditions to form elongated shapes: (i) $v_{imp} > 100$ m/s, (ii) $\theta_{imp} < 30°$, (iii) magnitude of shear velocity $v_{imp}\sin\theta_{imp} > 30$ m/s, and (iv) $M_{lr}/M_{target} > 0.4$. The qualitative meaning of each condition is as follows: (i) Elongation is the result of large deformation and thus large v_{imp} is required. (ii) Impacts with large θ_{imp} result in erosion of only edges of planetesimals. (iii) Elongated shapes are formed through stretch of planetesimals to the direction of shear velocity, so that large $v_{imp}\sin\theta_{imp}$ is also required. (iv) In largely destructive impacts, remnants are formed through rigorous reaccumulation and resultant shapes tend to be spherical.

The impact velocity considered in this study (50 m/s $< v_{imp} <$ 400 m/s) is relatively small compared to average collisional velocity in the main belt in the present solar system (about 5 km/s). Thus it is difficult to apply our result directly to the present solar system. However, in protoplanetaly disks impact velocities are small due to gas drag, and various irregular shapes might be formed during planet formation.

Although our present study is conducted with limited parameters (equal-mass impacts and relatively small impact velocities), more detailed relationship between impact conditions and resultant shapes will lead to reveal detailed history of the solar system.

References:

[1] Libersky L. D. and Petschek A. G. (1991) Lecture Notes in Physics, 395. [2] Benz W. and Ashaug E. (1995) Comput. Phys. Comm., 87, 253. [3] Jutzi M. (2015) Planet. Space. Sci., 107, 3. [4] Iwasawa M. et al. (2015) WOLFHPC'15, 1:1. [5] Iwasawa M. et al. (2016) Publ. Astron. Soc. Japan., 68 (4), 54. [6] Genda H. et al. (2012) Astrophis. J., 744, 137.